AD-A043 806   CALIFORNIA UNIV BERKELEY ELECTRONICS RESEARCH LAB   F/G 20/14
                SCATTERING OF ELECTROMAGNETIC WAVES BY BURIED DIELECTRIC BODIES--ETC(U)
                JUN 77   K K MEI, M E MORGAN, S K CHANG   DAAK02-75-C-0002

UNCLASSIFIED   NL

     | OF |
AD
A043 806

END
DATE
FILMED

9-77

DDC

(10)

SCATTERING OF ELECTROMAGNETIC WAVES BY
BURIED DIELECTRIC BODIES

Submitted by K. K. Mei

June 1977

D D C

SEP 6 1977

C

ELECTRONICS RESEARCH LABORATORY

College of Engineering

University of California, Berkeley

SCATTERING OF ELECTROMAGNETIC WAVES BY

BURIED DIELECTRIC BODIES,

by
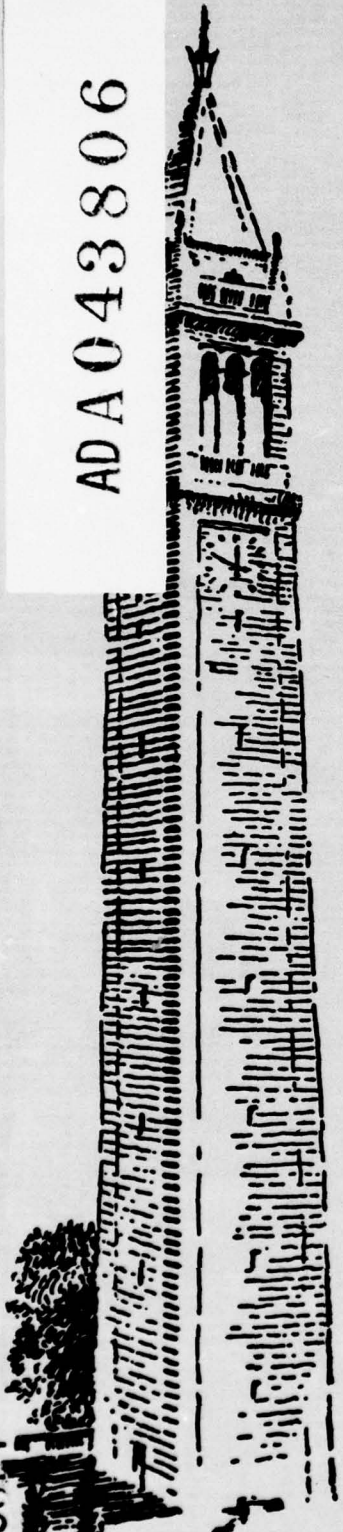
K. K. Mei, M. E. Morgan and S. K. Chang

Final Report, 1 Aug 74-30 Sep 77,

June 1977

57p.

DAAK02-75-C-0002

ELECTRONICS RESEARCH LABORATORY

College of Engineering
University of California, Berkeley
94720

127 550

FORWARD

The purpose of this investigation is to find the theoretical solutions to scattering of electromagnetic fields by dielectric bodies of revolution. This is the first part of the final goal of solving scattering by buried dielectric objects. The principal technique used in this investigation is the unimoment method which was developed for the purpose of solving scattering by dielectric bodies under contract DAAK02-71-C-0206. The application of this method to scattering by dielectric cylinders in a 2-dimensional space has been reported in the final report of the above contract. In this report, we shall extend the method to scattering in 3-dimensions. In the application of the unimoment method, one frequently has to deal with the finite difference or finite element method. In this report, we start with a discussion on these two methods regarding their differences and similarities. A method of inverting banded sparse matrix is also developed, and finally, the development of a special potential formulation of the Maxwell's equations for the axial symmetric problems, and the solution of the scattering problems.

FINITE METHODS IN ELECTROMAGNETIC SCATTERING

Kenneth K. Mei, Michael E. Morgan and Shu-Kong Chang

Department of Electrical Engineering and Computer Sciences
and the Electronics Research Laboratory
University of California, Berkeley, California 94720

ABSTRACT

Recent development in the unimoment method[1] has brought finite difference[2] and finite element methods[3] into the computational techniques of electromagnetic scattering. In this paper the various finite methods and their potentials in the scattering computations are examined. A section on programming technique is included for those uninitiated and the applications of the finite methods in 2-dimensional and 3-dimensional scattering problems, together with some of the associated computational subject matters are presented.

Introduction

Recent development in the unimoment method[1] has brought finite difference[2] and finite element methods[3] into the computational techniques of electromagnetic scattering. Finite difference had been a dominant computational method of solving partial differential equations, until it was overshadowed by the finite element methods in the mid-sixties. Recent development in sparse matrix algorithms has also changed the manner by which the finite methods are implemented. Originally, the relaxation methods were the main tools of solving finite difference equations, but now almost all finite equations are inverted instead of iteratively solved. The finite element method which was first developed by the structural engineers is now applied in almost all engineering disciplines. It is now well understood. Mathematical analysis[4] and sophisticated techniques[5,6] have been developed for it. In antenna and scattering computations the finite techniques are still like new found friends, and the acquaintance with them is yet to be developed. The purpose of this paper is to examine those methods from the stand point of one who is interested in electromagnetic scattering computations. A section on programming technique is included for those uninitiated and the applications of the finite methods in 2-dimensional and 3-dimensional scattering problems, together with some of the associated subject matters are presented.

Finite Methods

In this paper the term finite methods is meant to include finite difference, weighting function, Galerkin's and finite element (or Ritz finite element) methods. Literally any numerical method that approximates continum mathematics by discrete mathematics may be termed a finite method, however, that is not usually what we mean. For instance the moment method

of solving integral equations is not classified as a finite method. A finite method is traditionally used to solve differential or partial differential equations directly.

During the last fifteen years computation in electromagnetic scattering problems have been actively pursued almost entirely in terms of integral equations. Needless to say the drift to integral equation is very natural and for good reasons. In integral equations the computations are limited to the scatterer or antenna while in the finite methods they are generally spread over the entire space. In integral equations the radiation conditions are automatically satisfied while in the finite methods they require special numerical treatments which are often unsatisfactory. Recent advances in communications and remote sensing have urgently demanded the results of scattering by dielectric and lossy inhomogeneous bodies. The only practical approach to such problems appears to be direct solution of partial differential equations rather than solution by integral equation, the formulation of which in an inhomogeneous medium is already a difficult task. Recent development in the applications of finite methods[1] has essentially cleared the way for general applications of the finite methods in electromagnetic scattering.

For the sake of brevity we shall discuss the methods first in one dimension. Let $\mathcal{L}$ be a differential operator or more specifically for illustration we set $\mathcal{L} = \dfrac{d^2}{dx^2}$. The objective of the finite methods is to solve the equation

$$\mathcal{L}\phi(x) = f(x) \tag{1}$$

with boundary conditions $\phi(0) = a$
$$\phi(1) = b$$

-3-

In most numerical methods, the independent variable is discretized as shown in Fig. 1. The formulations of the finite methods are illustrated in the following:

$$\mathcal{L} = \frac{d^2}{dx^2}$$

Finite difference from fundamental meaning of derivative:

$$\frac{\phi_{i+1} - 2\phi_i + \phi_{i-1}}{(\Delta x)^2} = f_i \qquad i = 1, \ldots, N-2 \tag{2}$$

Weighting function method I (WFM I)

$$\int_0^1 \frac{d^2 \phi(x)}{dx^2} W_i(x) dx = \int_0^1 f(x) W_i(x) dx \qquad i = 1, 2 \ldots M \tag{3}$$

Weighting function method II (WFM II) (Integration by parts of WFM I)

$$\phi'(x) W_i(x) \Big]_0^1 - \int_0^1 \frac{d\phi}{dx} \frac{dW_i}{dx} dx = \int_0^1 f(x) W_i(x) dx \tag{4}$$

Galerkin's method

$$\phi(x) = \sum_{i=1}^{N} a_i \zeta_i(x) \text{ and set } W_i(x) \text{ in (4) to } \zeta_i(x)$$

(Ritz) Finite Element

$$\text{Minimize } I = \int_0^1 [(\frac{d\phi}{dx})^2 + 2f\phi] dx \tag{5}$$

In most text books the weighting function methods are not distinguished by whether integration by parts is used or not. For convenience of the following discussion we shall call it weighting function method II when integration by parts is used, otherwise weighting function method I.

We shall name the set of functions which are used to approximate the solution $\phi(x)$ the trial functions, thus

$$\phi(x) = \sum_{i=1}^{N} a_i \zeta_i(x) \tag{6}$$

where ζ_i are trial functions. $W_i(x)$ are a set of weighting functions.

The following are a few definitions of commonly used terms:

patch function - functions which are zero outside an element and its close neighbors, such as those shown in Fig. 2.

element - a line segment (one dimension), area (two dimension) or volume (three dimension) as a result of discretization.

interpolate - a set of trial functions is termed interpolative if it is unity at one node and zero at all other nodes. An interpolative trial function has the property that

$$\phi(x) \approx \sum_{i=1}^{N} a_i \zeta_i(x)$$

where a_i represents $\phi(x_i)$.

conformity - a set of trial functions is termed conforming if each of its members is continuous.

Only those methods that use patch functions as trial functions and weighting functions will be considered as finite methods.

It is well-known that the finite difference equations are derived from Taylor's series. It is not difficult to relate the finite difference equation to the W.F. method. Consider a quadratic patch function

$$Q_i(x) = A_i + B_i(x - x_i) + C_i(x - x_i)^2 \tag{7}$$

passing through $\phi(x_{i-1})$, $\phi(x_i)$, $\phi(x_{i+1})$. It is immediately evident

$$A_i = \phi(x_i); \quad B_i = \frac{\phi(x_{i+1}) - \phi(x_{i-1})}{2\Delta x}; \quad C_i = \frac{\phi(x_{i+1}) - 2\phi(x_i) + \phi(x_{i-1})}{2(\Delta x)^2}.$$

In (3) let $\phi(x) = \sum_{i=1}^{N} Q_i(x)$, the weighting functions $W_i(x)$ be

$\delta(x - x_i)$, and we find that (3) reduces to the finite difference equation (2).

On the other hand, in (5) let $\phi(x) = \sum_{i=1}^{M} a_i \zeta_i(x)$

$$I = \int_0^1 \{ [\sum_{i=1}^{M} a_i \xi_i{}'(x)]^2 + 2f \sum_{i=1}^{M} a_i \xi_i(x) \} dx$$

$$\frac{\partial I}{\partial a_j} = \int_0^1 \{ 2[\sum_{i=1}^{M} a_i \xi_i{}'(x)] \xi_j{}'(x) + 2f \xi_j(x) \} dx = 0$$

$$j = 1, 2, \ldots M \qquad\qquad (8)$$

which is equivalent to (4) if the trial functions $\xi_i(x)$ and the weighting

functions $W_i(x)$ are the same set of functions, and $W_1(0) = W_M(1) = 0$.

Numerical restrictions

While W.F. method I and II seem to be only a simple mathematical

step away from each other, their numerical constraints are quite different.

In the simple example of Eqs. (3) and (4), it is evident that in W.F.

method I the trial functions must be at least Quadratic and the weighting

functions be integrable; while in W.F. method II, the trial functions can

be linear and the weighting function must belong to C', (W'(x) integrable).

The consequence is: one can use linear functions as trial functions in

W.F. method II, but not in method I.

Another important observation is that the union of the set of trial

functions must cover the entire region, while the weighting functions are

not so required. Thus, in the W.F. methods, the weighting functions may

be sampling functions e.g. pulses or patch functions which do not overlap,

such as shown in Fig. 3 as opposed to those patch functions of Fig. 2

which are used as trial functions.

One important property of sampling is that discrepancies in the trial functions may be suppressed by the weighting functions. An obvious discrepancy in the W.F. method I using piecewise quadratic trial functions is that the trial functions are not conforming, as illustrated in Fig. 4. If we use the left of the quadratic for $x_i - \frac{\Delta x}{2} \leq x \leq x_i + \frac{\Delta x}{2}$ and the right quadratic for $x_{i+1} - \frac{\Delta x}{2} \leq x \leq x_{i+1} + \frac{\Delta x}{2}$, the discontinuity is obvious. Yet it causes no ill effect because the weighting functions are zero at the discontinuities.

The case of discontinuity becomes very serious for the finite element method, since the trial functions are now chosen to be the weighting functions and the union of trial functions must cover the entire region. The derivatives at the discontinuities result in delta functions, and the square of delta functions are not integrable. That is why elements must be conforming in the finite element method. However, being non-conforming may still not be fatal in the finite element method. Frequently the irregularities are ignored and the computations still may yield good results, although just as frequently they may fail. Nonconforming elements are often referred to as "variational crime" in finite element literatures, and there exists a test, known as the "patch test," which may be used to predetermine whether a specific set of non-conforming elements would converge to the correct result. In one dimension, conforming elements are easily obtained even for high order polynomial approximations. Any piecewise polynomial function, which is non-zero at only one node is a conforming element. In two or more dimensions conforming requires extra effort, which may result in increasing the number of nodes or the band of the matrix or both.

One Dimension Finite Methods

Consider the W.F. method II using linear functions for both $\xi_i(x)$ and $W_i(x)$ such as those shown in Fig. 2a. The integral in (4) from x_{i-1} becomes

$$\int_{x_{i-1}}^{x_i} \frac{\phi_i - \phi_{i-1}}{\Delta x} \cdot \frac{1}{\Delta x} \, dx - \int_{x_{i-}}^{x_{i+1}} \frac{\phi_{i+1} - \phi_i}{\Delta x} \cdot \frac{1}{\Delta x} \, dx$$

$$= - \frac{\phi_{i+1} - 2\phi_i + \phi_{i-1}}{\Delta x} \tag{9}$$

which is almost identical to the finite difference equation (2) except that the right hand side of (2) is collocation and that of (4) is weighted by a linear patch function. Indeed the base of the weighting function may be reduced without any effect on the equation.

Now, consider a quadratic trial function used in W.F. method II, i.e.,

$$\xi_i(x) = \phi_i + \frac{\phi_{i+1} - \phi_i}{2\Delta x} (x - x_i) + \frac{\phi_{i+1} - 2\phi_i + \phi_{i-1}}{2 \, \Delta x^2} (x - x_i)^2$$

$$\tag{10}$$

then,

$$\frac{d\xi_i(x)}{dx} = \frac{\phi_{i+1} - \phi_i}{2\Delta x} + \frac{\phi_{i+1} - 2\phi_i + \phi_{i-1}}{\Delta x^2} (x - x_i) \tag{11}$$

If the weighting function is even with respect to x_i, $\frac{dW_i}{dx}$ will be odd function w.r.t. x_i, thus the first term in (11) will have no contribution in the integral of the product $\frac{d\xi_i(x)}{dx} \frac{dW_i(x)}{dx}$, and we shall get an equation again identical to the finite difference equation.

It seems that all finite methods can be reduced to the same equations. The fact is that, in this particular example, the second order polynomial operated on by the differential operator results in a constant. As a result,

for this example a sampling weighting function set is as good as any distributed weighting function set. Indeed, the quadratic functions are the best approximation functions one can get to solve this particular problem, because the differential equation is satisfied not only at the nodes but also between nodes, and any attempt to use higher ordered approximations usually makes the approximation worse rather than better.

Two Dimensional Problems

The above is the story for one-dimensional equations. In two dimensions many of the above discussions are still valid, but there are other complications.

(A) Conformity

Conformity of elements in one dimension is never a problem, but in two-dimensions it is a major problem when high order approximations are to be considered. Consider a typical finite element discretization in Fig. 5. The elements are triangular and the trial functions are pyramidal like linear patch functions. Obviously a visual representation of the relation between our trial functions and the problem geometry requires the use of one additional dimension. A typical trial function consists of 6 elements and 7 nodes. Referring to Fig. 5, a linear trial function centering at the point i, consists of six planes which have values one at the point i and 0 at the other nodes, such as shown in Fig. 6.

It is evident that the linear elements are conforming, i.e., any linear combination of such trial functions shall have no discontinuity.

The second order approximation in the finite element methods uses a piecewise quadratic function for $\phi(x,y)$ within each element,

$$\phi(x,y) = a_0 + a_1 x + a_2 y + a_3 xy + a_4 x^2 + a_5 y^2 \tag{12}$$

The quadratic function of (x,y) has six degrees of freedom. The

three nodes of a triangular element are not sufficient to determine the

six coefficients of the quadratic. Extra nodes need to be added, such

as shown in Fig. 7, in which a node is designated on each side of an

element. These trial functions are now conforming. Quadratics which are

unity at one node and zero at the rest of the nodes of a triangular

element can be found either by inverting a 6 x 6 matrix or by using an

area coordinate system (for details see refs. [5], [7].) The second order

approximation in the finite element method gives better accuracy but it

also increases the number of nodes and increases the bandwidth of the

matrix.

In finite difference assuming square mesh, the usual five point

equation for the Laplacian operator gives, (referring to Fig. 5)

$$\phi_{i+N} + \phi_{i+1} - 4\phi_i + \phi_{i-1} + \phi_{i-N} = 0 \tag{13}$$

It is a result of quadratic approximation of $\phi(x,y)$ near ϕ_i, but it is

not a complete quadratic. Indeed, a five point equation cannot represent

a complete quadratic which has six coefficients. The missing term in

(13) is a_3 x y, which can be omitted if the mesh is rectangular.

The trial functions result in (13) are not conforming but the

discrepancy is again suppressed by the weighting functions. Again, for

solving Laplace's equation, the quadratic equation of (13) satisfies

the differential equation between nodes along the mesh, and it should be

a better approximation than the nine point finite difference equations

(fourth order polynomial) which satisfies the differential equation only

at the nodes. Many engineers have been surprised to find that their

nine point finite difference equations give worse results than the

five point finite difference equations when dealing with Laplace's equation.

(B) Consistency

Because of the sampling property of the finite difference equations, there are frequent inconsistancies, particularly when dealing with inhomogeneous media. In the case of a Helmholtz equation for a continuously inhomogeneous medium, the finite difference equation is,

$$\phi_{i+N} + \phi_{i+1} + (k_i^2 h^2 - 4\phi_i) + \phi_{i-1} + \phi_{i-N} = 0 \qquad (14)$$

where the field points ϕ_{i+N}, ϕ_{i+1}, ϕ_i, ϕ_{i-1}, ϕ_{i-N} are assumed to be in a homogeneous medium ε_i. Let i be replaced by i + 1, we find ϕ_i, ϕ_{i+1} are now assumed to be in a homogeneous medium ε_{i+1}. This type of inconsistency, while tolerable, is not very satisfying theoretically. The problem becomes more serious when a node is situated at a material discontinuity such as shown in Fig. 8. There are several ways of handling material discontinuities in the finite difference method but in general they are not satisfying.

In the finite element method, the fields are clearly identified in each patch, hence there is no ambiguity like that of the finite difference. Furthermore, the quadratic functions in the finite element are piecewise quadratic and a typical trial function actually consists of six piecewise quadratic functions, while in the finite difference method the requirement of twice differentiability on the trial functions necessitates a single polynomial to cover a group of connected nodes.

(C) Flexibility

Because the polynomials in the finite elements method are complete, the method is essentially independent of the shape of the triangular element. In the finite difference method, the polynomial is incomplete,

hence it is restricted to rectangular meshes. It can be made to be
independent of mesh geometry, however, by using a six point difference
mesh such as shown in Fig. 9. Indeed, for a six point finite difference,
since it is now independent of mesh geometry, the mesh is no longer
needed. The only requirement is that the nodes are relatively uniformly
distributed. A survey of recent developments in variable grid finite
difference methods can be found in Ref. [8].

The usual applications of the finite difference method use rectangular
mesh, with the boundary nodes specially treated by extrapolation or
interpolation.[9] The merit of such a shceme is the simplified programming,
and the disadvantage is reduced accuracy and the difficulties involved
in finding the normal derivatives from the solution. In the finite element
method, using triangular elements, it is necessary to store information
about the locations of the nodes, and also the information about the elements,
i.e., the nodes which form a particular element. Finite difference
methods using variable mesh should require the same information, i.e.,
the information about the neighboring nodes of a control node must be
available. Consequently, finite difference method using variable
mesh is about as flexible as the finite element method, and the degree
of complexity in programming for both methods are about the same.

The conclusion is that the finite difference method is about as good
as linear approximation in the finite element method. The higher order
approximation in the finite element method should be more accurate than
the corresponding approximations in the finite difference method, yet the
finite element method would require more nodes. The finite difference
method using a rectangular grid is simple to program but less flexible, and by

using star meshes it can be made more flexible but its complexity is raised to that of the linear finite element method. The method not very often used is the W.F. method II, with which one may use piecewise polynomial trial functions as in the finite element method yet with a much relaxed conformity requirement. It will be a worthwhile project to investigate whether the relaxed conformity requirement on W.F. method II can reap some of the benefits of higher order approximations without increasing the nodes or bandwidth of the resulting matrix.

Programming Technique

To implement the finite methods one need first to describe the geometry and construct the mesh, followed by generating the matrix and solving the matrix. These basic steps are described in the following:

(1) Mesh Construction

In most practical problems, the node numbers are large and the mesh topology is complicated. Therefore, it is almost an impossible task to instruct the computer in an exact mesh geometry. The best strategy is to construct a rule which the program can follow to generate the mesh automatically. There are many ways of automatic mesh generation. In the following we shall describe one of them, which we have used very effectively:

(a) Construct a regular mesh inside the circular boundary

This can be done in many ways a few of which are shown in Fig. 10. These mesh can be generated automatically. Fig. 10(a) is used if the center part of the circle is included. Fig. 10(c) is used when the center part of the circle is not included in the finite method.

-13-

(b) <u>Find the intersections of the scatterer contour with the mesh</u>
     <u>line</u>

If the mathematical formula of the scatterer contour is known, it
is relatively easy to find the intersections of the contour with the
mesh lines. For the mesh geometry of Fig. 10(c) it is a particularly
easy task, because we only need to find the intersections between the
contour and the radial lines. One of the two nearest nodes to an
intersection point along the radial line is now shifted to the intersection
point. The rest of the nodal points along the particular radial lines
are now shifted so as to make the perturbation equally distributed. It
is noticed that there are two possible orientations of the diagonal
hypotenuse of the triangular elements between two adjacent radial lines.
We shall call those elements of Fig. 11a, left handed (LH) elements and
those of Fig. 11b, right handed (RH) elements. The choice on the type
of element may be made based on the rule,

$$R_{i+1} \geq R_i \Rightarrow \text{LH element}$$

$$R_{i+1} < R_i \Rightarrow \text{RH element}$$

Using the above rules, the contour of a distorted raindrop is discretized
in Fig. 12.

(2) Computation of Matrix Elements

The key to the programming of any finite method with variable elements
is the name list of nodes, which form a particular element. Referring to
Fig. 13, we generate an array ELEM(I,J), where I, is the numbering of the
element and the dimension for J is three. This array is used to store
the list of the nodes which form the particular element I. For example,
ELEM(12,1) = 3; ELEM(12,2) = 6, ELEM(12,3) = 7. Of course, the coordinate

-14-

locations of each node should be stored in another array.

With the information of the elements and nodes available, we now consider the generation of the matrix elements. In the following, we shall consider the generation of the matrix element of the two-dimensional Helmholtz equation using the weighting function method II. Thus we compute the integral,

$$\int_S (\nabla U \cdot \nabla W_i + k^2 U W_i) ds \tag{15}$$

Both U and W will be piecewise linear functions, therefore the result will be identical to the finite element method.

A typical linear element h, with nodes $(h)_1$, $(h)_2$, $(h)_3$ should have the field within the element described by a linear function,

$$U_{(h)} = a_{(h)1} + a_{(h)2}x + a_{(h)3}y \tag{16}$$

The coefficients $a_{(h)i}$ are found by matrix inversion,

$$\bar{a}_{(h)} = N_{(h)}^{-1} \bar{U}_{(h)} \tag{17}$$

The vector $\bar{U}_{(h)}$ consists of the field at the nodal points hence $U_{(h)i}$, (i = 1,2,3), and

$$N_{(h)} = \begin{bmatrix} 1 & x_{(h)1} & y_{(h)1} \\ 1 & x_{(h)2} & y_{(h)2} \\ 1 & x_{(h)3} & y_{(h)3} \end{bmatrix} \tag{18}$$

Let us consider W_i to be a linear pyramid function which is unity at node i and zero at the surrounding six nodes, such as shown in Fig. 14. Throughout the entire process of weighting integrals, each element will be weighted by three different weighting functions, each of which may be represented

by a linear function which is unity at one node of the element and zero at the other two. The function which is unity at node (h)i is actually part of the weighting function (h)i, and the coefficients generated by it are associated with the (h)ith equation or the (h)ith row of the matrix.

To each $U_{(h)}$ in an element h, there are three associated weighting functions $W_{(h)j}$ (j = 1, 2, 3). Let $W^j_{(h)}$ be part of $W_{(h)j}$ which is associated with the element h and which has value at the node (h)j and zero at the other two nodes of element h.

$$W^j_{(h)} = b^j_{(h)1} + b^j_{(h)2}x + b^j_{(h)3}y \qquad (18)$$

and

$$\bar{b}^j_{(h)} = N^{-1}_{(h)} \bar{n}_j$$

where

$$\bar{n}_1 = \begin{bmatrix} 1 \\ 0 \\ 0 \end{bmatrix} , \quad \bar{n}_2 = \begin{bmatrix} 0 \\ 1 \\ 0 \end{bmatrix} , \quad \bar{n}_3 = \begin{bmatrix} 0 \\ 0 \\ 1 \end{bmatrix}$$

The gradient of $U_{(h)}$ gives;

$$\nabla U_{(h)} = \begin{bmatrix} 0 & 0 & 0 \\ 0 & 1 & 0 \\ 0 & 0 & 1 \end{bmatrix} \begin{bmatrix} a_{(h)1} \\ a_{(h)2} \\ a_{(h)3} \end{bmatrix} = \begin{bmatrix} 0 & 0 & 0 \\ 0 & 1 & 0 \\ 0 & 0 & 1 \end{bmatrix} N^{-1}_{(h)} \bar{U}_{(h)} \qquad (19)$$

and the gradient of $W^j_{(h)}$ is,

$$\nabla W^j_{(h)} = \begin{bmatrix} 0 & 0 & 0 \\ 0 & 1 & 0 \\ 0 & 0 & 1 \end{bmatrix} N^{-1}_{(h)} \bar{n}_j \qquad (20)$$

The integral $\int_{(h)} \nabla U_{(h)} \cdot \nabla W^j_{(h)} \, ds$ is,

$$\int_{(h)} \bar{U}_{(h)}^T \begin{bmatrix} 0 & 0 & 0 \\ 0 & 1 & 0 \\ 0 & 0 & 1 \end{bmatrix} N^{-1}_{(h)}{}^T \begin{bmatrix} 0 & 0 & 0 \\ 0 & 1 & 0 \\ 0 & 0 & 1 \end{bmatrix} N^{-1}_{(h)} \bar{n}_j \, ds$$

$$= \bar{U}_{(h)}^T \cdot \bar{P}^j_{(h)} A_{(h)} \qquad (21)$$

-16-

where $A_{(h)}$ is the area of the element h, and $\bar{p}^j = [p^j_{(h)1}, p^j_{(h)2}, p^j_{(h)3}]^T$.
$A_{(h)} p^j_{(h)i}$ is recognized as the contribution to the matrix element
$G[(h)j, (h)i]$ $(i = 1, 2, 3)$. This value should be accumulated in the array
G in the location $G[(h)j, (h)i]$.

Simularly the second integral of (15) can be carried out by

$$k^2 \int_{(h)} U_{(h)} W^j_{(h)} ds = k^2 \int_{(h)} \bar{U}^T_{(h)} N^{-1}_{(h)}{}^T \begin{bmatrix} 1 \\ x \\ y \end{bmatrix} [1 \ x \ y] N^{-1}_{(h)} \bar{n}_j ds$$

(22)

$$= k^2 \int_{(h)} \bar{U}^T_{(h)} N^{-1}_{(h)}{}^T \begin{bmatrix} 1 & x & y \\ x & x^2 & xy \\ y & xy & x^2 \end{bmatrix} N^{-1}_{(h)} \bar{n}_j \ ds$$

$$= k^2 \int \bar{U}^T_{(h)} \cdot \bar{q}^j_{(h)} \ ds$$

(23)

The ith element of the vector $\bar{q}^j_{(h)}$ is thus the contribution to the $(h)j^{th}$
row and $(h)i^{th}$ column of the matrix. The integrals

$$I_{ij} = \int_{(h)} x^i y^j ds$$

(24)

may be found by using the local coordinates,

$$u = x - x_c$$

$$v = y - y_c$$

$$x_c = (x_{(h)1} + x_{(h)2} + x_{(h)3})/3$$

$$y_c = (y_{(h)1} + y_{(h)2} + y_{(h)3})/3$$

The following table gives the most useful results [10]:

$i + j$	I_{ij}
0	A (area of triangle)
1	0
2	$\frac{A}{12}(u_1^i v_1^i + u_2^i v_2^j + u_3^i v_3^j)$
3,4	$\frac{A}{30}(u_1^i v_1^j + u_2^i v_2^j + u_3^i v_3^j)$
5	$\frac{2A}{105}(u_1^i v_1^j + u_2^i v_2^j + u_3^i v_3^j)$

where $u_i = x_{(h)i} - x_c$

$\qquad v_i = y_{(h)i} - y_c$

and

$\qquad A = |\det N_{(h)}|/2$

If $k^2 = k_0^2 \epsilon$ where $\epsilon(x,y)$ is a function of position, we may represent $\epsilon(x,y)$ by piecewise polynomial functions, and the integrals can be found accordingly.

(3) Solving the linear equations

The dimension of the unknown vector $\bar{u}$ is usually very large. Fortunately the matrix $G(I,J)$ is usually sparse and banded. Referring to Fig. 13, we notice that the nodes $(1,2,3,4)$ are only connected to the interior nodes $(5,6,7,8)$ which are only connected to the interior $(1,2,3,4)$ and $(9,10,11,2)$ etc. Representing these nodal values of the field by vectors,

-18-

$$\bar{v}_1 = (u_1, u_2, u_3, u_4)$$

$$\bar{v}_2 = (u_5, u_6, u_7, u_8)$$

$$\bar{v}_3 = (u_9, u_{10}, u_{11}, u_{12})$$

$$\bar{v}_4 = (u_{13}, u_{14}, u_{15}, u_{i6})$$

we can represent the banded matrix by the vector equations

$$B_i \bar{v}_{i-1} + A_i \bar{v}_i + C_i \bar{v}_{i+1} + \bar{d}_i = 0 \tag{25}$$

The matrix equation is thus, (referring to Fig. 13)

$$G\bar{U} = \begin{bmatrix} A_1 & C_1 & 0 & 0 \\ B_2 & A_2 & C_2 & 0 \\ 0 & B_3 & A_3 & C_3 \\ 0 & 0 & B_4 & A_4 \end{bmatrix} \begin{bmatrix} \bar{v}_1 \\ \bar{v}_2 \\ \bar{v}_3 \\ \bar{v}_4 \end{bmatrix} = \begin{bmatrix} \bar{d}_1 \\ \bar{d}_2 \\ \bar{d}_3 \\ \bar{d}_4 \end{bmatrix} \tag{26}$$

where all A_i's are 4 x 4 sparse matrices, C_i's are lower triangular sparse matrices (frequently diagonal) and B_i's are upper triangular sparse matrices (frequently diagonal); $B_1 = C_4 = 0$ and the vector $\bar{d}_i$ represent the contributions from the boundary values.

The solution can be obtained by the following block-by-block elimination method. Assume

$$\bar{v}_{i-1} = R_i \bar{v}_i + \bar{s}_i \qquad i = 1, 2, \ldots \tag{27}$$

Eq. (25) can be rewritten as

$$\bar{v}_i = -(A_i + B_i R_i)^{-1} C_i \bar{v}_{i+1} - (A_i + B_i R_i)^{-1} (B_i \bar{s}_i + \bar{d}_i) \tag{28}$$

Comparing (28) with (27) with i = i+1, we get

$$R_{i+1} = - (A_i + B_i R_i)^{-1} R_i \qquad (29)$$

and

$$\bar{s}_{i+1} = - (A_i + B_i R_i)^{-1} (B_i \bar{s}_i + \bar{d}_i) \qquad (30)$$

The above two recurrence formulas can be initiated with i = 1 in Eq. (25), which results in

$$\bar{v}_1 = -A_1^{-1} c_1 \bar{v}_2 - A_1^{-1} \bar{d}_1 \qquad (31)$$

Comparing (31) with Eq. (27) for i = 2, we get

$$\left. \begin{array}{l} R_2 = -A_1^{-1} C_1 \\ \bar{s}_2 = -A_1^{-1} \bar{d}_1 \end{array} \right\} \qquad (32)$$

Comparing (32) with (29) and (30), it is clear that

$$\left. \begin{array}{l} R_1 = 0 \\ s_1 = 0 \end{array} \right\} \qquad (33)$$

The end condition at i = N is

$$B_N \bar{v}_{N-1} + A_N \bar{v}_N + \bar{d}_N = 0 \qquad (34)$$

Substituting Eq. (27), with i = N, into (34) we get,

$$\bar{v}_N = - (A_N + B_N R_N)^{-1} (B_N \bar{s}_N + d_N) = \bar{s}_{N+1} \qquad (35)$$

To summarize, we have the following procedure:

(I)   Use the initial conditions (33)

(II) To generate R_i, $\bar{s}_i$ (i = 1,2,...,N+1) from the recurrence
      formulas (29) and (30).

-20-

(III) Use the end condition (35)

(IV) To calculate $\bar{v}_i$ (i = N, N-1, N-2,...,1) from (27).

Applications

(A) Two Dimensional Scattering

Equation (29) clearly indicates that all the R_i matrices can be computed independent of the boundary values. Therefore, we may obtain a set of the solutions of the interior problem based on a set of specified boundary values from the same R_i's. The vectors $\bar{s}_i$'s are dependent on the boundary values but their computations are not as time consuming as those for R_i's. From the interior solutions the normal derivatives for each Dirichlet problem can be found.

Let the exterior solution be expanded in a finite series of cylindrical harmonics, assuming symmetry with respect to the x-axis,

$$u(\bar{r}) = \sum_{n=0}^{N} a_n \cos n\phi \, H_n^{(2)}(kr) \qquad r \geq a \qquad (36)$$

and the interior solution be expanded into N + 1 linearly independent solutions described in the previous section,

$$u(\bar{r}) = \sum_{n=0}^{N} b_n u_n(\bar{r}) \qquad r \leq a \qquad (37)$$

where $\underline{a}$ is the radius of the circumscribing circle, and the normal derivatives $\frac{\partial U_n}{\partial r}$ (a) are found via the solutions $u_n(\bar{r})$. To find the coefficients a_n and b_n, we equate (36) and (37), and their normal derivatives at r = a, to get

$$\int_0^{\pi/2} \{U^{in}_{(a,\phi)} + \sum_{n=0}^{N} a_n \cos n\phi \, H_n^{(2)}(ka)\} \cos m\phi \, d\phi$$

$$= \sum_{n=0}^{N} b_n \int_0^{\pi/2} U_n(a,\phi) \cos m\phi \, d\phi \quad (m = 0,1,2,\ldots,N) \tag{38}$$

$$\int_0^{\pi/2} \{\frac{\partial U^{inc}}{\partial r}(a,\phi) + \sum_{n=0}^{N} a_n \cos n\phi \frac{\partial H_n^{(2)}}{\partial r}(ka)\} \cos m\phi \, d\phi$$

$$= \sum_{n=0}^{N} b_n \int_0^{\pi/2} \frac{\Delta U_n(a,\phi)}{\Delta r} \cos m\phi \, d\phi \quad (m = 0,1,\ldots,N) \tag{39}$$

The above should result in a $2(N+1) \times 2(N+1)$ matrix from which the coefficients can be found. A word of advice here regarding the normal derivatives $\frac{\partial U^{inc}}{\partial r}(r)$ and $\frac{\partial H_n^{(2)}}{\partial r}(kr)$. In general, the exact values of the normal derivatives of the incident field and the Hankel's functions are known on $r = a$, however, it is advisable to use their approximate values $\frac{\Delta U^{inc}}{\Delta r}(a)$ and $\frac{\Delta H_n^{(2)}}{\Delta r}(a)$ instead. The reason is that the right side of (39) contains approximate derivatives obtained from the finite difference of the nodal values. They are not equal to the exact derivatives. The equality of the approximate and the exact derivatives can be enforced in (39) only through the alteration of the coefficients from their proper values. Indeed, equation (39) is more meaningful if both sides have the same order of approximation.

A few solutions of the 2-dimensional scattering are shown in Fig. 15-16. The details of the 2-dimensional solution can be found in Ref. [3].

(B) Three Dimensional Scattering

(1) Formulation

A truly arbitrary three dimensional scattering problem of reasonable

-22-

size is not going to be solved economically in the foreseeable

future using any presently available technique. The three dimensional

scatterers that can be investigated reasonably economically are axially

symmetrical. An axially symmetrical scatterer with non-axially symmetric

incident fields can be decomposed into azimuthal modes,

$$\bar{E}(\rho,z,\phi) = \sum_{m=-\infty}^{\infty} \bar{e}_m(\rho,z)e^{jm\phi} \tag{40}$$

$$\eta_0\bar{H}(\rho,z,\phi) = \sum_{m=-\infty}^{\infty} \bar{h}_m(\rho,z)e^{jm\phi} \tag{41}$$

where η_0 = 120π ohms. We shall use the cylind cal coordinates for the

interior problem instead of spherical coordinates so that the integrals

resulting from the finite methods will be more manageable. The above

azimuthal components can be solved independently of one another.

Let R = kρ and Z = kz, and $\psi_{m,1}$ and $\psi_{m,2}$ be the two scalar potentials,

$$\frac{\psi_{m,1}}{R} = \hat{\phi} \cdot \bar{e}_m \tag{42}$$

$$\frac{\psi_{m,2}}{R} = \hat{\phi} \cdot \bar{h}_m \tag{43}$$

The rest of the field components can be derived from the potentials

by the following formulas:[9]

$$\hat{\phi} \times \bar{e}_m = jf_m(m\hat{\phi} \times \nabla\psi_{m,1} - R\mu_r\nabla\psi_{m,2}) \tag{44}$$

$$\hat{\phi} \times \bar{h}_m = jf_m(m\hat{\phi} \times \nabla\psi_{m,2} + R\epsilon_r\nabla\psi_{m,1}) \tag{45}$$

where

$$f_m = [\mu_r(R,Z)\epsilon_r(R,Z)R^2 - m^2]^{-1} \tag{46}$$

-23-

The differential equations of $\psi_{m,1}$ and $\psi_{m,2}$ are

$$\nabla \cdot [f_m(R\epsilon_r \nabla\psi_{m,1} + m\hat{\phi} \times \nabla\psi_{m,2})] + \epsilon_r\psi_{m,1}/R = 0 \tag{47}$$

$$\nabla \cdot [f_m(R\epsilon_r \nabla\psi_{m,2} - m\hat{\phi} \times \nabla\psi_{m,1})] + \mu_r\psi_{m,2}/R = 0 \tag{48}$$

These differential equations can be recast into the minimization of the functional,

$$F = \int_S L(R,Z,\psi_1,\psi_2,\nabla\psi_1,\nabla\psi_2)dRdZ \tag{49}$$

where

$$L = f_m[\nabla\psi_{m,1} \cdot (R\epsilon_r \nabla\psi_{m,1} + m\hat{\phi} \times \nabla\psi_{m,2}) + \nabla\psi_{m,2}(R\mu_2\nabla\psi_{m,2} - m\hat{\phi} \times \nabla\psi_{m,1})]$$

$$- (\epsilon_r\psi_{m,1}^2 + \mu_r\psi_{m,2}^2)/R \tag{50}$$

It is noticed that $f_m(R,Z)$ is singular at the surfaces where $R\sqrt{\mu_r\epsilon_r} = |m|$. This can happen when μ_r and ϵ_r are both real. The nodal fields do not, however, behave erratically at these surfaces and, in fact, except at points which correspond to material interfaces, the modal field components are uniformly holomorphic.

(2) Singular Integrals

In the application of finite methods to (47) and (48) or (50) the singular integrals of the type,

$$Q_{r,s} = \int_\Omega \frac{R^2 Z^s}{\epsilon_r \mu_r R^2 - m^2} dRdZ \tag{51}$$

are often encountered. The integration of (51) may be effected as follows:

-24-

Consider the integral

$$I = \int_{\Omega} g(R) Z^s dR dZ .$$ (52)

Using the two dimensional Stoke's theorem,

$$\int_{\Omega} \nabla \times \bar{v} \cdot \overline{ds} = \oint_{\partial \Omega} \bar{v} \cdot \overline{d\ell} ,$$ (53)

and letting

$$\bar{V}(R,Z) = - \frac{g(R) Z^{s+1}}{s+1} \hat{R} ,$$ (54)

we have

$$\nabla \times \bar{v} = -g(R) Z^s \hat{\phi} \quad \text{and} \quad \overline{ds} = -\hat{\phi} dR dZ$$

and (53) becomes

$$\int_{\Omega} g(R) Z^s dR dZ = \frac{1}{s+1} \oint_{\partial \Omega} g(R) Z^{s+1} dR .$$ (55)

Applying (55) to (51) we get

$$Q_{r,s} = \frac{1}{s+1} \oint_{\partial \Omega} \frac{R^r Z^{s+1}}{\epsilon_r \mu_r R^2 - m^2} dc .$$ (56)

For a typical element the clockwise contour of (56) is shown in Fig. 17. Consider a typical integration along a line segment, such as from the ith node to the jth node. Along this path the linear functional dependence of $Z(R) = \alpha R + \beta$ where

$$\alpha = \frac{(Z_j - Z_i)}{(R_j - R_i)} \quad \text{and} \quad \beta = Z_i - \alpha R_i$$ (57)

is substituted into the integrand of (56), and the term $Z^{s+1} = (\alpha R + \beta)^{s+1}$ is expanded into binomial series in powers of R. The resultant integrals will be of the form,

-25-

$$I_Q(n,m) = \int_{R_i}^{R_j} \frac{R^n}{k^2 R^2 - m^2} \, dR \tag{58}$$

where $n = 0, 1, \ldots, r + s + 1$, for $n = 0, 1$ we have

$$I_Q(0,m) = \begin{cases} -(k^2 R)^{-1} \Big|_{R_i}^{R_j}, & m = 0 \\[2ex] \dfrac{1}{2km} \{\ln(kR - m) - \ln(kR + m)\} \Big|_{R_i}^{R_j}, & m \neq 0 \end{cases} \tag{59}$$

$$I_a(1,m) = \frac{1}{2k^2} [\ln(kR - m) + \ln(kR + m)] \Big|_{R_i}^{R_j} \quad \text{all } m \tag{60}$$

The remainder of the integrals may be generated using the recurrence formula

$$I_Q(n,m) = I_Q(n,0) + \frac{m^2}{k^2} I_Q(n - 2, m) . \tag{61}$$

An important result to be noted is the fact that even for the case of lossless media, where $k = \sqrt{\varepsilon_r \mu_r}$ is real, the quadrature in I_Q will produce complex values when the integration passes through the simple pole singularity in the integrand. The pole locations for the case of real and complex k are illustrated in Fig. 18, and hence the integration path deformation necessary for real k, where $\delta \to 0$. In pathing through the pole, with increasing R, the appropriate natural log function in (59) and (60) will pick up an additional $j\pi$ to add to the integral, which is contributed by the residue of the integral. The Global System matrix, will thus include complex elements even in the lossless media case.

Results

Using the above described formulas and computational techniques, we are able to compute the scattering of plane waves by dielectric bodies of revolution of various shapes.[10] To verify the computed results we first compute the scattering by a dielectric sphere, the exact result of which is known. In the computations, we deliberately off set the center

-26-

of the scatterer from the origin, so that computationally speaking
the geometry is no longer regular. The comparison of the results is
shown in Fig. 19 for the scattering amplitude and Fig. 20 for the phase.

As computational techniques becomes more sophisticated, verification
of the computed results soon becomes a problem, because classical solutions
of a few special geometries will not be sufficient to confirm the computations
of complex problems. Experimental verification may eventually be the only
way to confirm the validity of general programs. We have both computed
and measured the bistatic scattering of a finite dielectric cylinder with
a spherical void in the center such as shown in Fig. 21. The computed
and measured results are shown in Fig. 22 and 23. Their agreement is
truly remarkable. These results should definitively confirm the applicability
of the unimoment method in electromagnetic scattering problems.

Further development

At the present using linear finite elements methods, it is possible
to solve axially symmetrical dielectric scattering problems which have a
maximum dimension of about $4\lambda_0$, using the CDC 7600 computer. Actually
it is difficult to be exact regarding the limitation of the method because
it should depend on the dielectric constant and geometry of the scatterer.
At this stage, however, it is quite evident that the immediate limitation
of the method is the capacity of the computer in handling finite element
equations in a large closed region. Fortunately, finite element techniques
have been extensively investigated by structural engineers and improvements
of these techniques have been reported at each of the related conferences.
The finite element technique described in this paper is quite elementary.
Yet, with this elementary approach, we have already extended the art of

scattering computation quite significantly. It is conceivable that more sophisticated finite methods could enhance the dimensions of solvable interior problems to the point that the size of the matrix, resulting from enforcing the continuity conditions on the separable surface, becomes the limiting factor of the computation. Therefore, the most needed effort is to exploit the power of the finite element method and to popularize its use among the electromagnetic community.

The application of the technique is very broad indeed. Current problems, such as, scattering by advanced composite, materials absorption by biological material, scattering by buried obstacles, just to name a few, can all be analyzed with finite methods. It is also conceivable that the unimoment method can be combined with the method of moments to solve a variety of problems, which consist of wires and bodies of revolution.

In conclusion, we would like to emphasize that the application of finite methods in antenna and scattering problems is not an alternative to the method of moment, rather it is its supplement. It is obvious that the finite method is most uneconomical where the method of moments is most economical, such as in thin wire problems, whereas the finite method is most attractive where the method of moments is most clumsy, such as scattering by inhomogeneous material bodies.

References

[1] Mei, K. K. "Unimoment method of solving antenna and scattering problems," IEEE Trans. Antennas and Propagat., Vol. Ap-22, pp. 760-766, Nov. 1974.

[2] Stovall, R. K. and K. K. Mei, "Application of a unimoment technique to a biconical antenna with inhomogeneous dielectric loading," IEEE Trans. on Antennas and Prop. Vol. Ap-23, No. 3, May 1975.

[3] Chang S. K. and K. K. Mei, "Application of the unimoment method to electromagnetic scattering of dielectric cylinders," IEEE Trans. Antennas and Prop., Vol. Ap-24, No. 1, pp. 35-42, Jan. 1976.

[4] Strang, G. and G. J. Fix, An analysis of the finite element method, Englewood Cliff, N. J., Prentice Hall, 1973.

[5] Zienkiewicz, O. C. and Y. K. Cheung, The Finite Element Method in Structural and Continuum Mechanics, London: McGraw Hill, 1967.

[6] Wachspress, E. L. A Rational Finite Element Basis, Academic Press, 1975.

[7] Norrie, D. H., and G. DeVries, The Finite Element Method, Academic Press, New York, 1973.

[8] Jensen, P. S., "A survey of some recent work in variable grid finite difference methods for partial differential equations," Lockheed Missles and Space Co., Palo Alto, Calif., Report LMSC 6-78-70-24 (1970) 12pp.

[9] Morgan, M., S. K. Chang and K. K. Mei, "Coupled azimuthal potentials for electromagnetic field problems in inhomogeneous axially-symmetric media," to be published in IEEE Trans. and Antennas and Prop. Mar. 1977.

[10] Morgan, M. "Numerical computation of electromagnetic scattering
      by inhomogeneous dielectric bodies of revolution," Ph.D. Thesis,
      Department of Electrical Engineering and Computer Sciences,
      University of Calif., Berkeley, 1976.
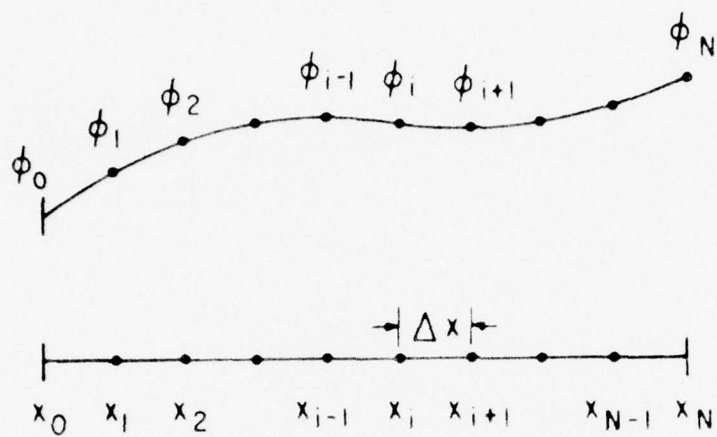
Fig. 1. Discretization of an independent variable
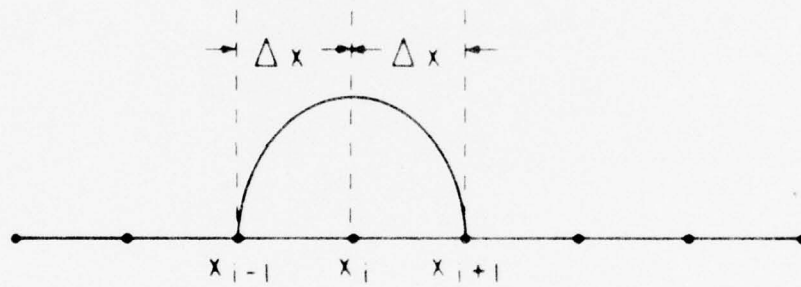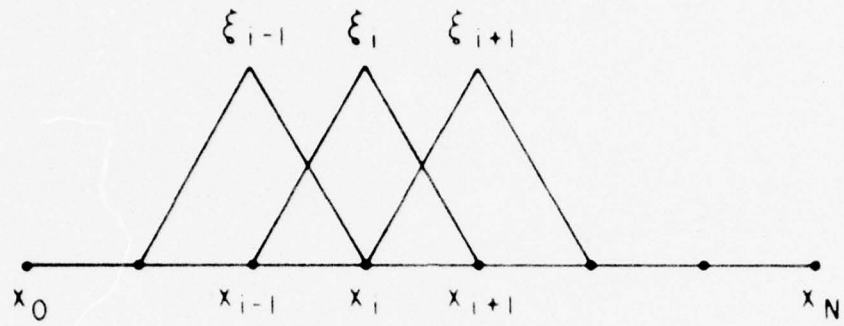
$$1 \quad - \quad \frac{(x - x_i)^2}{\Delta x^2}$$

Fig. 2. Patch functions (a) Linear (b) quadratic.
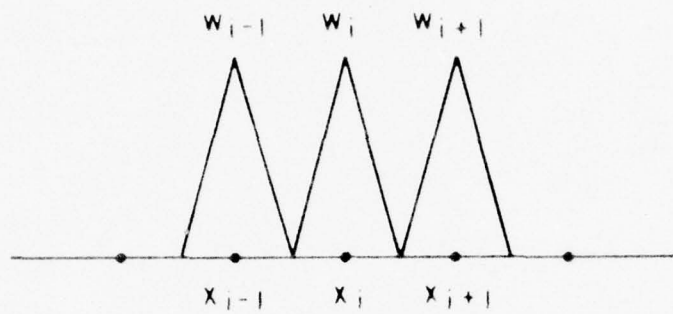
Fig. 3. Patch functions which can only be used as weighting functions.
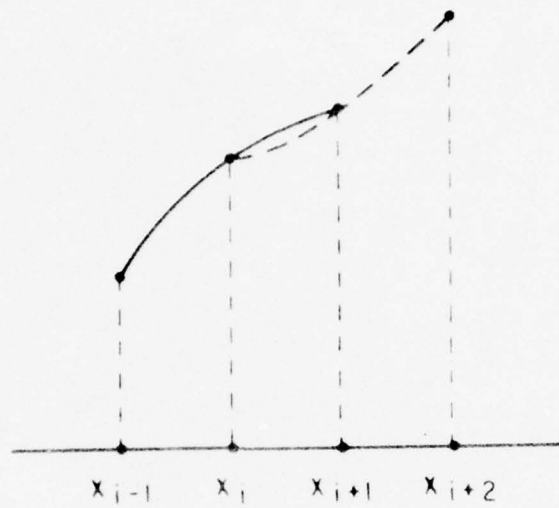
Fig. 4. Nonconforming trial functions.
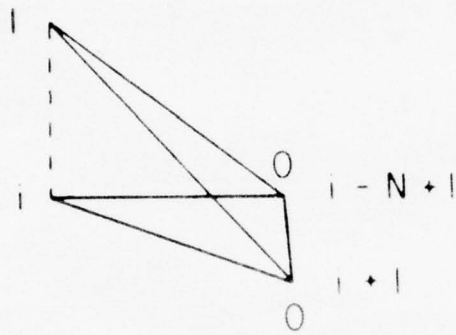
Fig. 6. A typical linear trial function for 2-dimensional finite element method.
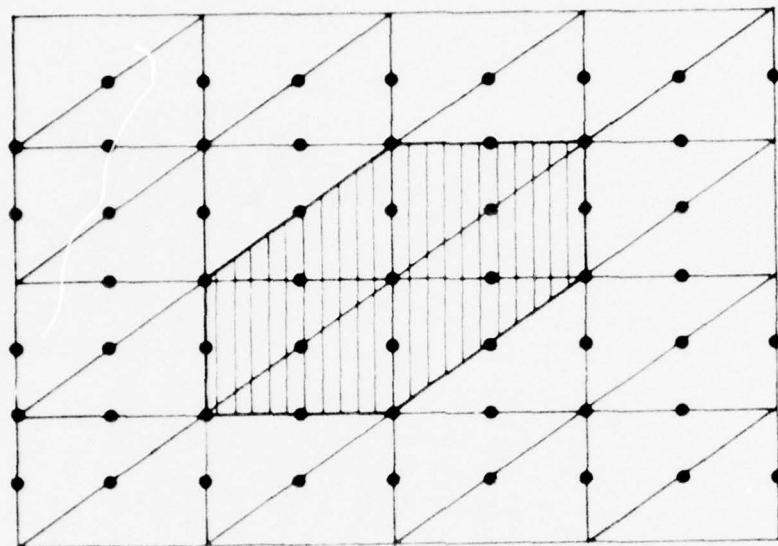
Fig. 7. Discretization and nodes for quadratic elements in a 2-dimension finite element method.
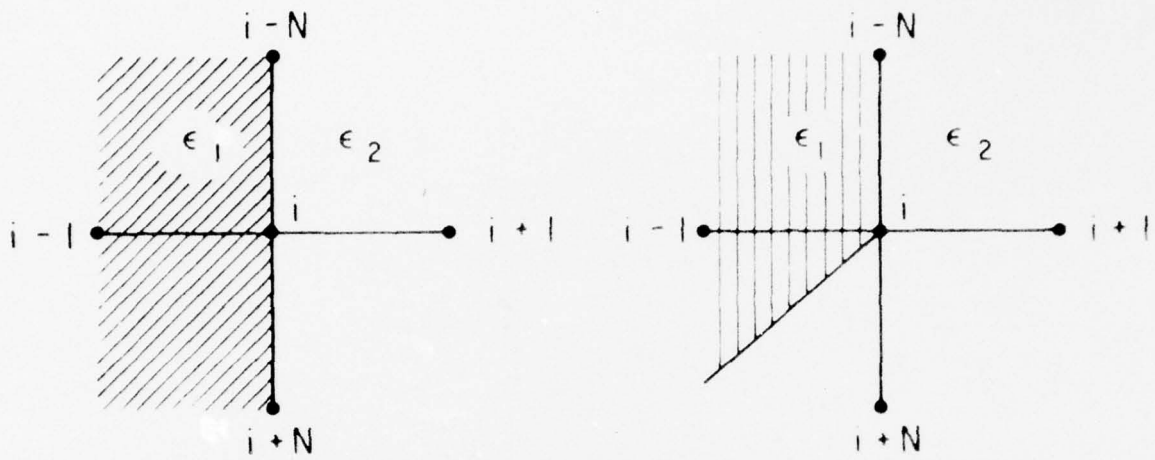
Fig. 8. Nodes on material discontinuities.
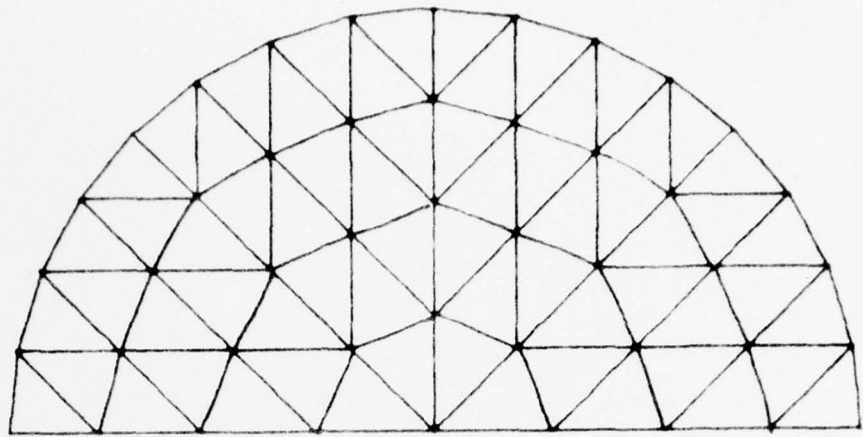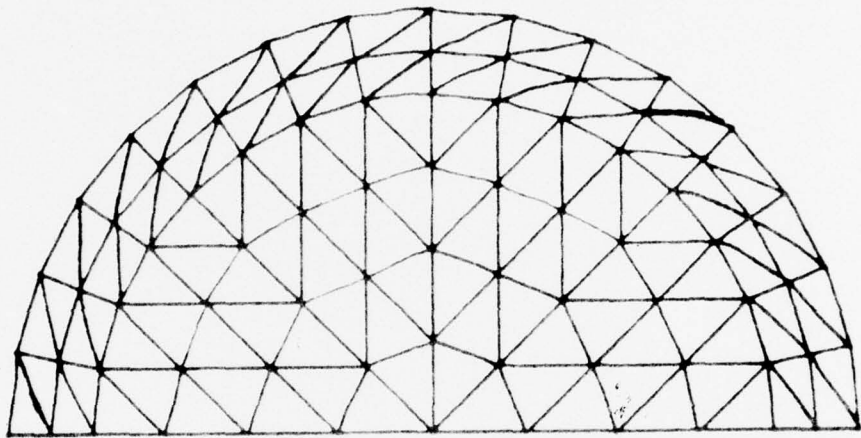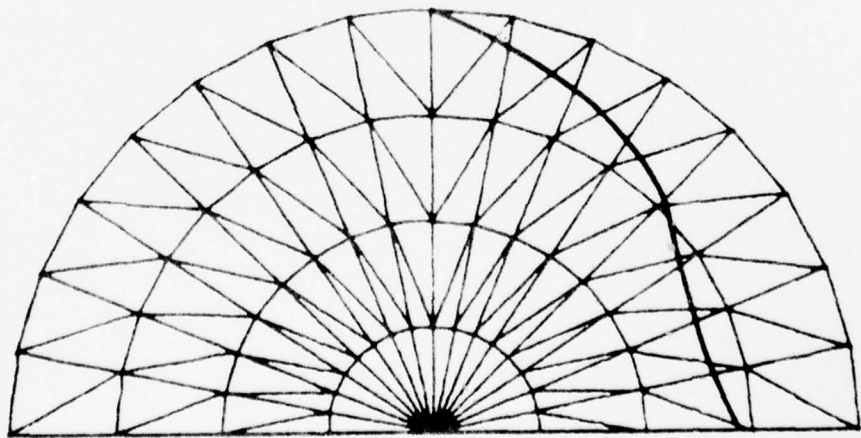
Fig. 10. Regular meshes in a circular region.
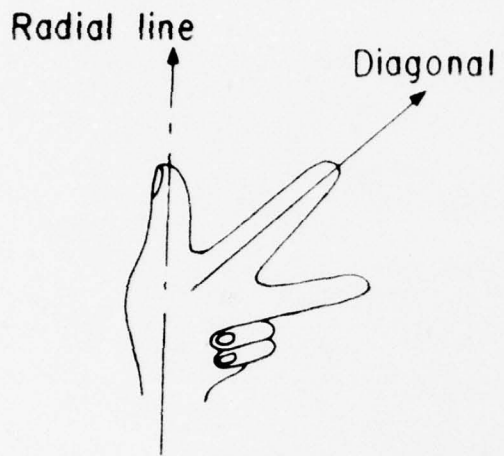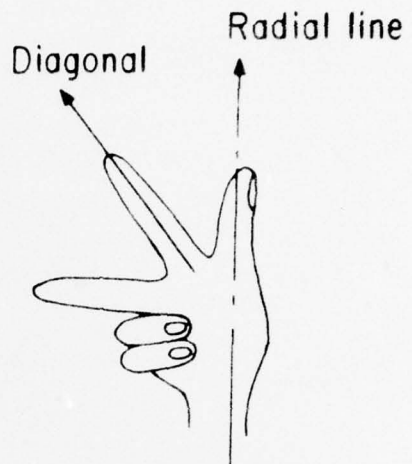
Fig. 11. (a) Left handed and (b) right handed elements.

Raindrop Surface
of Revolution
$R_{max} \approx 0.5$ cm
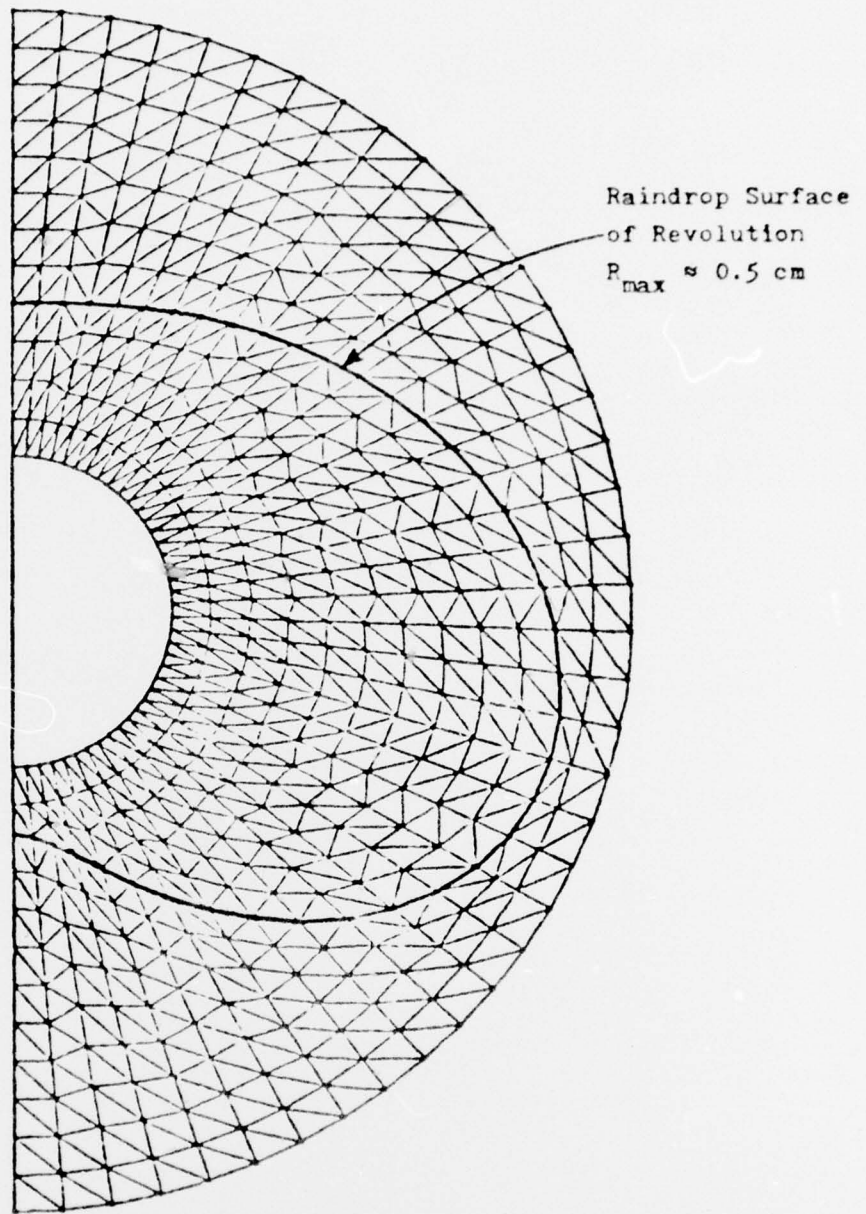
Fig. 12. Discretization of a distorted raindrop.
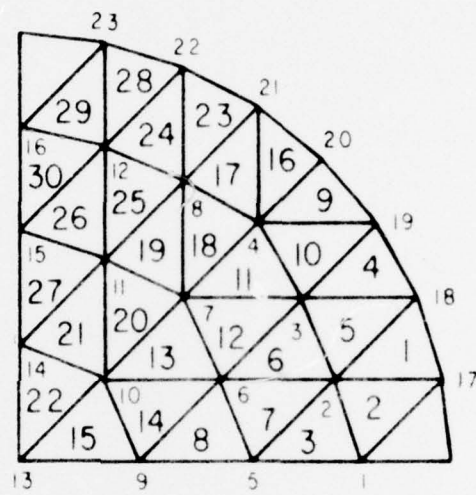
Fig. 13. An example of element and node numbering.

-43-
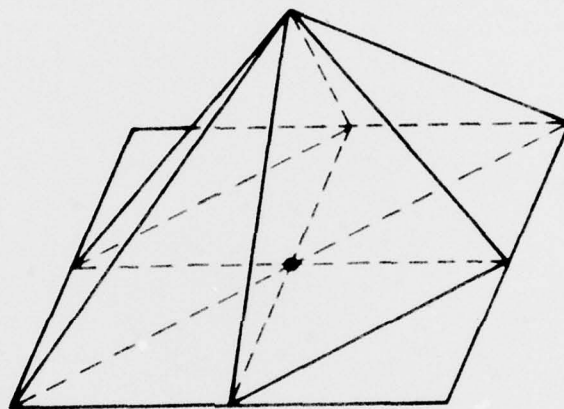
Fig. 14. A linear weighting function.
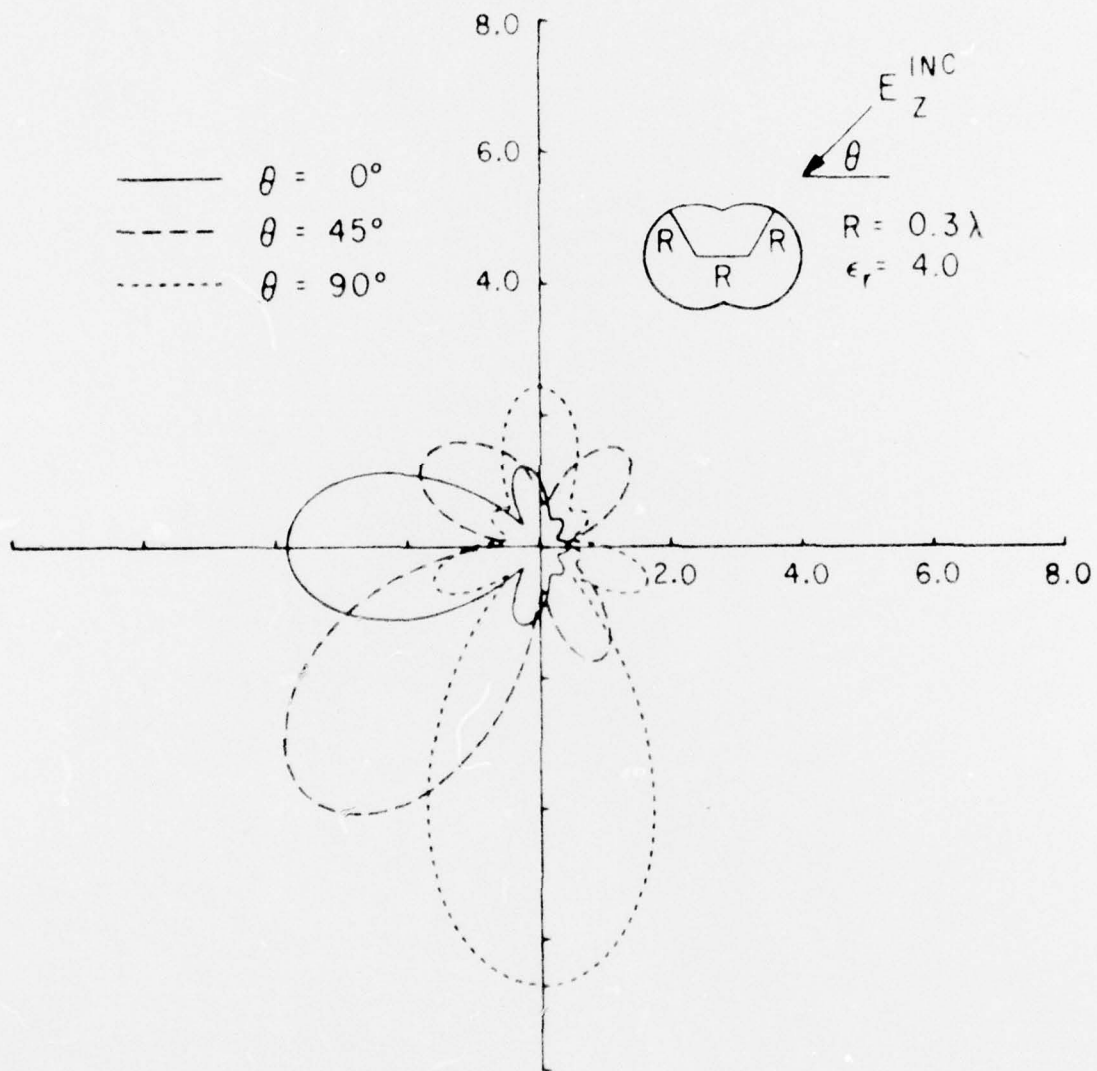
Fig. 15. Scattering by two overlapping dielectric cylinders; E_z^{inc}.
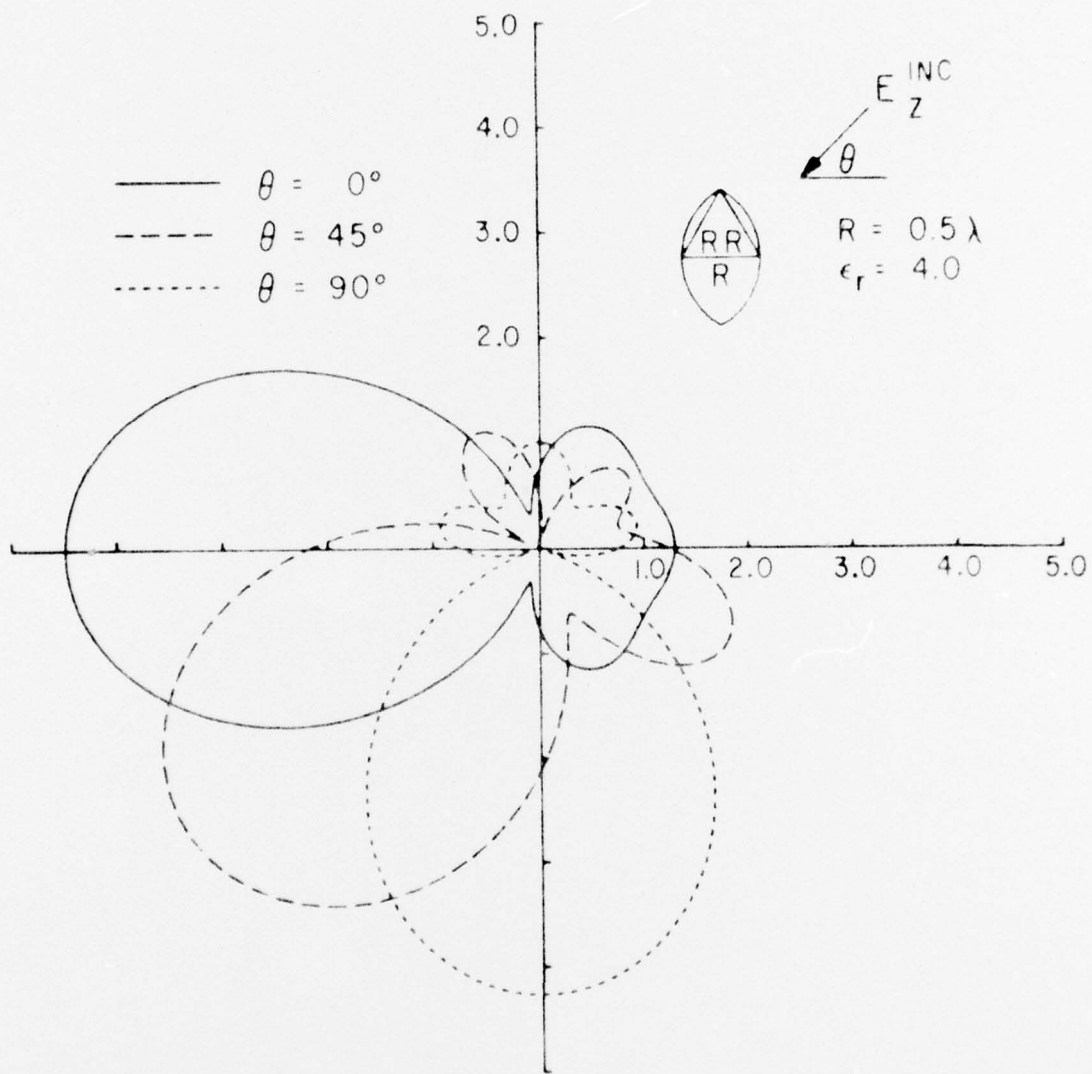
Fig. 16. Scattering by a lens.

-46-
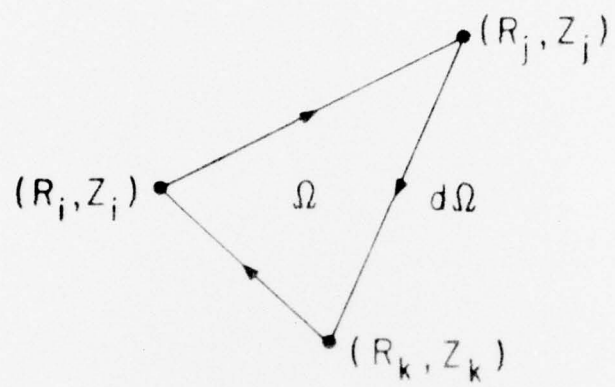
Fig. 17. A contour integral around an element.
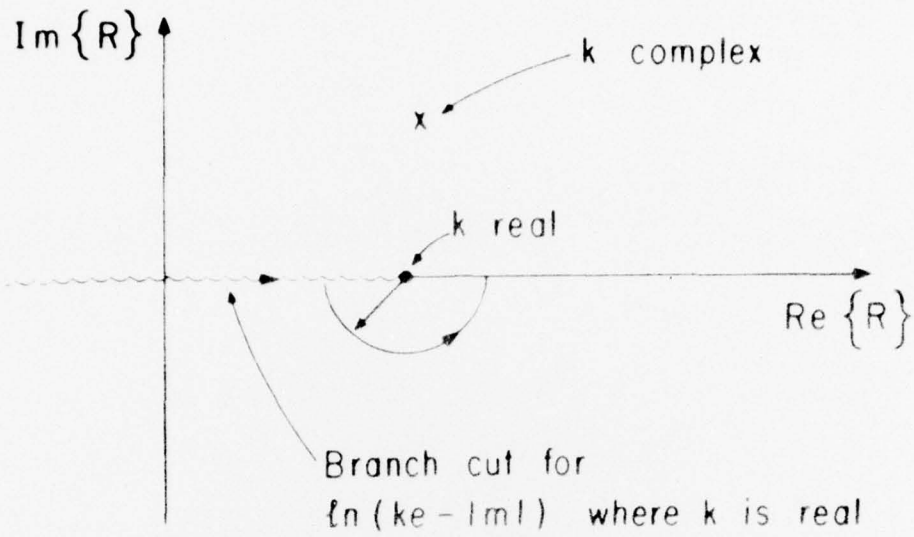
Fig. 18. The pole locations of real and complex k.
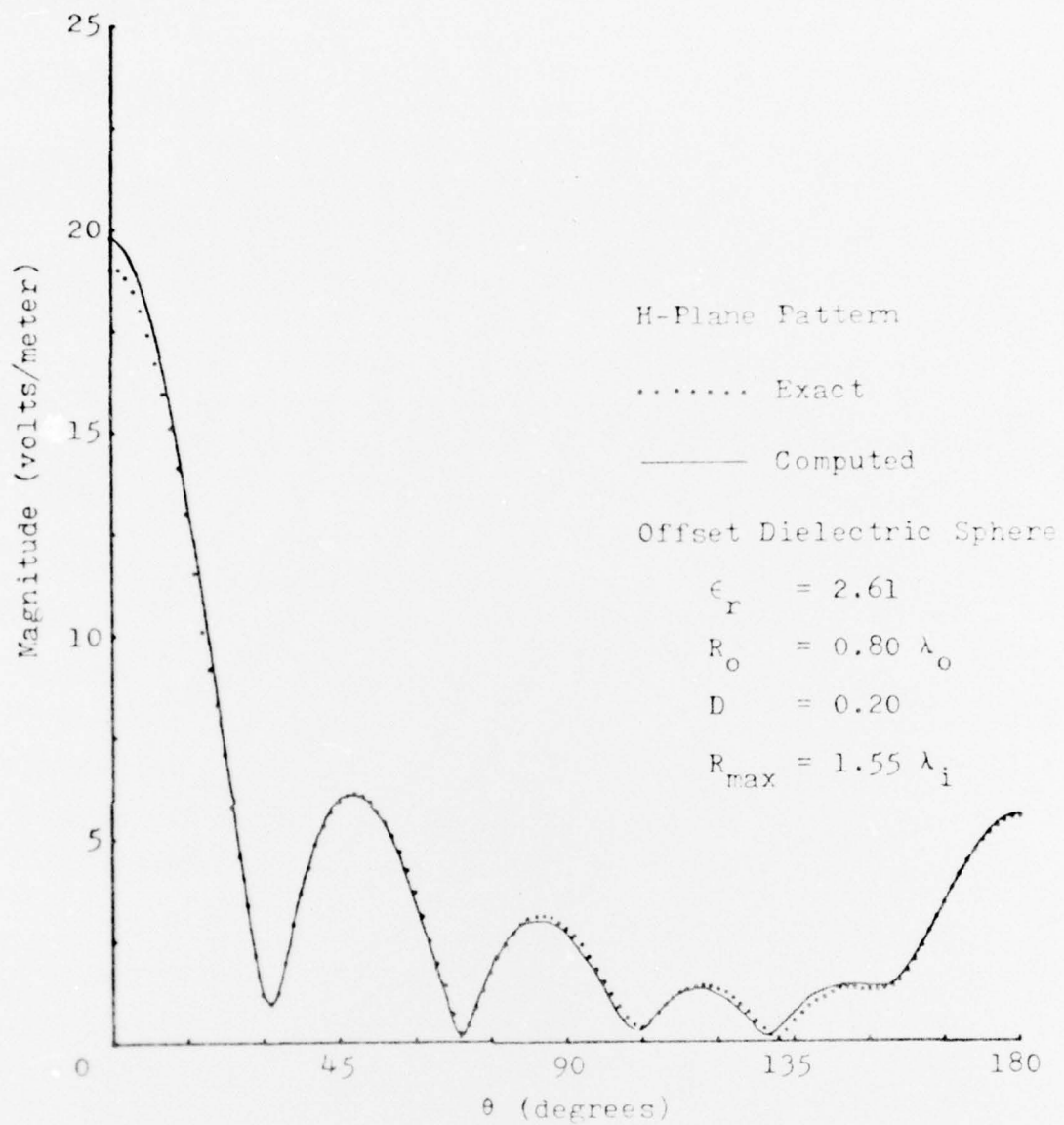
Fig. 19. The comparison of amplitudes of scattered fields by numerical
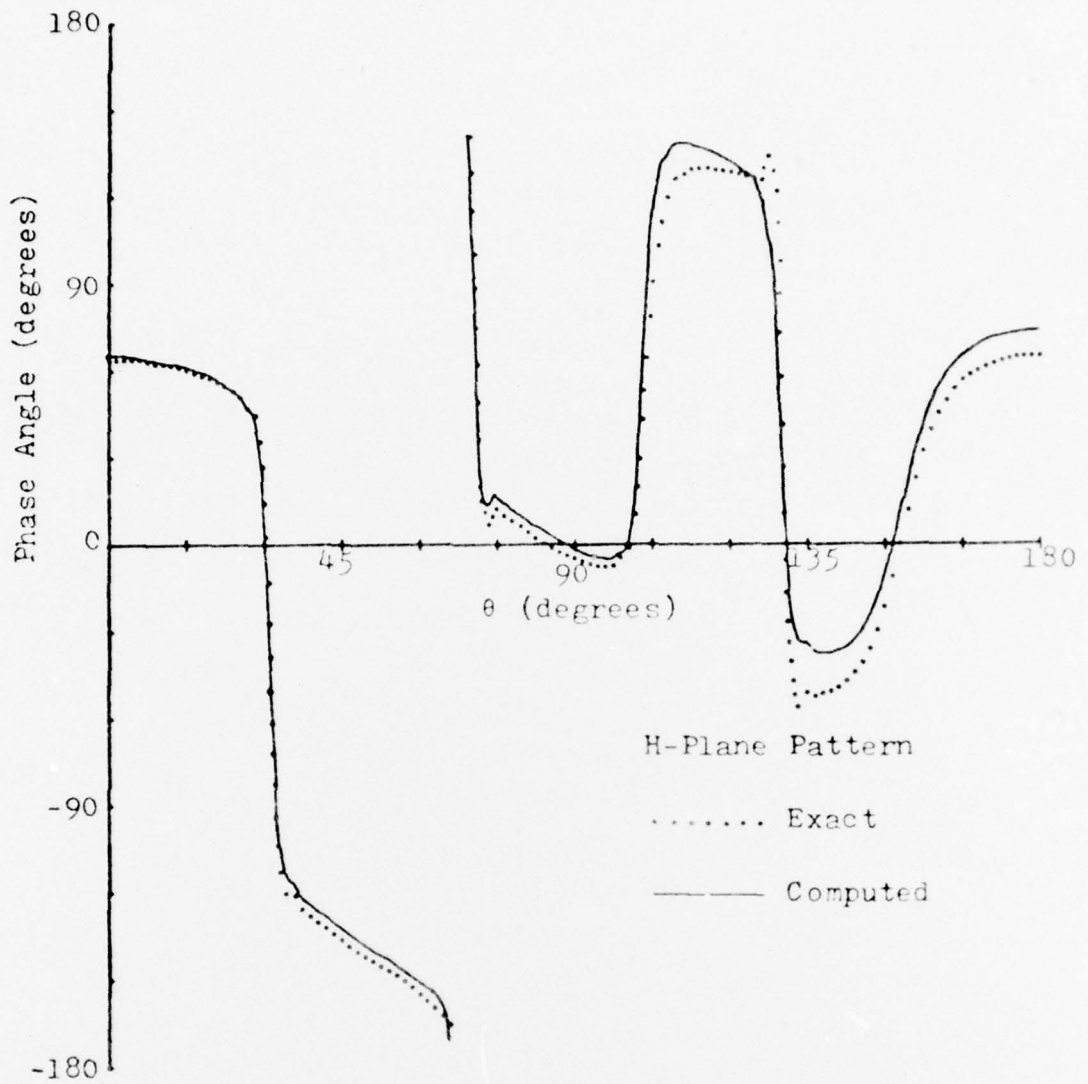and analytical solutions of a dielectric sphere.

Fig. 20.   The comparison of phases of scattered fields by numerical and analytical solutions of a dielectric sphere.
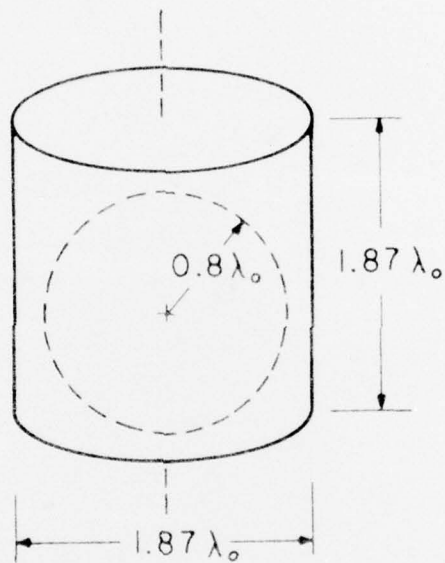
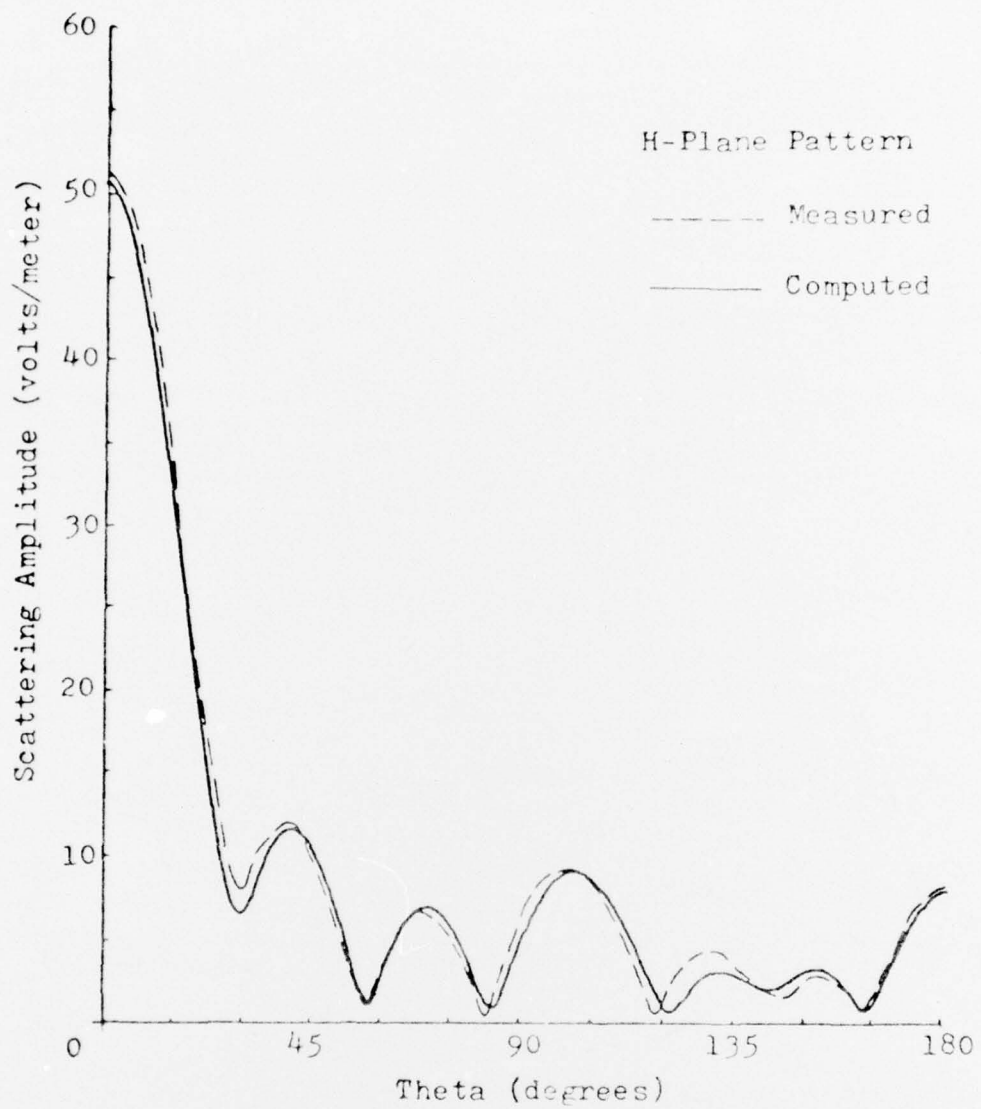Fig. 21. A dielectric finite cylinder with a spherical void.

Fig. 22.   Computed and measured amplitudes of scattered fields of a
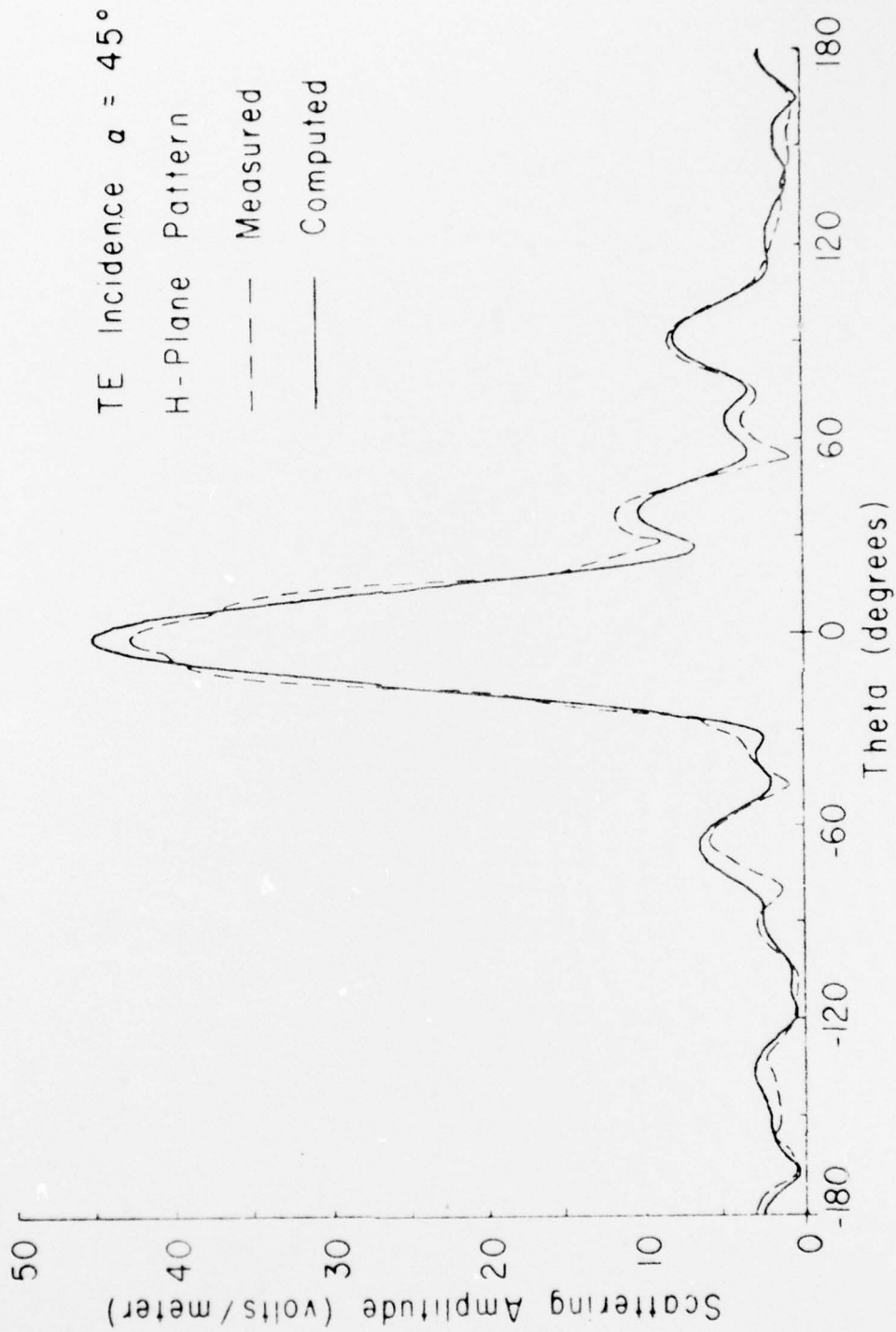hollow dielectric cylinder illuminated by a 90° incident plane
wave.

Fig. 23. Same as Fig. 22 with a 45° incident plane wave incident plane wave.

-53-

REPORT DOCUMENTATION PAGE		READ INSTRUCTIONS BEFORE COMPLETING FORM
1. REPORT NUMBER	2. GOVT ACCESSION NO.	3. RECIPIENT'S CATALOG NUMBER
4. TITLE (and Subtitle) Scattering of Electromagnetic Waves by Buried Dielectric Bodies		5. TYPE OF REPORT & PERIOD COVERED FINAL 8/1/74-9/30/77
		6. PERFORMING ORG. REPORT NUMBER
7. AUTHOR(s) K. K. Mei, M. E. Morgan and S. K. Chang		8. CONTRACT OR GRANT NUMBER(s) DAAK02-75-C-0002
9. PERFORMING ORGANIZATION NAME AND ADDRESS Electronics Research Laboratory University of California Berkeley, California 94720		10. PROGRAM ELEMENT, PROJECT, TASK AREA A WORK UNIT NUMBERS
11. CONTROLLING OFFICE NAME AND ADDRESS Dept. of the Army U.S. Army Mobility Equip. Res. & Devel. Command Fort Belvoir, VA 22060		12. REPORT DATE
		13. NUMBER OF PAGES
14. MONITORING AGENCY NAME & ADDRESS(if different from Controlling Office)		15. SECURITY CLASS. (of this report) UNCLASSIFIED
		15a. DECLASSIFICATION/DOWNGRADING SCHEDULE

16. DISTRIBUTION STATEMENT (of this Report)

Approved for public release; distribution unlimited

17. DISTRIBUTION STATEMENT (of the abstract entered in Block 20, if different from Report)

NA

18. SUPPLEMENTARY NOTES

19. KEY WORDS (Continue on reverse side if necessary and identify by block number)

Finite Difference, Finite Element, Electromagnetic Scattering, Unimoment
Method, Computation, Coupled Azimuthal Potential, Dielectric Scattered,
body of revolution, pentrable body, Lossy scatterer

20. ABSTRACT (Continue on reverse side if necessary and identify by block number)

Recent development in the unimoment method has brought finite difference
and finite element methods into the computational techniques of electromagnetic
scattering. In this paper the various finite methods and their potentials in
the scattering computations are examined. A section on programming technique
is included for those uninitiated and the applications of the finite methods
in 2-dimensional and 3-dimensional scattering problems, together with some of
the associated computational subject matters are presented.

DD FORM 1473 EDITION OF 1 NOV 65 IS OBSOLETE
1 JAN 73